

Electroformation of Microlayers of Ionic Liquids in Undiluted Nitromethane and Its Homologues. Unusual Oscillations behind the Range of Limiting Steady-State Current

Karolina Caban, Mikolaj Donten, and Zbigniew Stojek*

Department of Chemistry, Warsaw University, Pasteura 1, PL-02-093, Poland

Received: September 3, 2003; In Final Form: November 10, 2003

Steady-state limiting currents for the electroreduction of undiluted nitromethane and two other nitroalkanes are easily obtained by voltammetry and chronoamperometry at Pt microelectrodes. Since the electrode process is one-electron and the counterion is tetraalkylammonium cation, it is concluded that microlayers of ionic liquid of the stoichiometry $\text{ANO}_2^-\text{R}_4\text{N}^+$ are formed at the microelectrode surface, where R denotes either $-(\text{CH}_2)_3\text{CH}_3$ or $-(\text{CH}_2)_5\text{CH}_3$ and A stands for the appropriate alkane. The results of gravitational and temperature experiments indicate that the ionic layer is more viscous and less dense compared to pure corresponding nitroalkane. Behind the potential range of the limiting steady-state current, at potentials more negative than -6 V vs Pt quasi-reference electrode, unusual, very reproducible oscillations are formed. These oscillations are thought to be related either to the upward gravitational movement of microdrops of the ionic liquid formed or the electroreduction of the counterion and consecutively to periodical changes in the true electrode potential of the Pt microelectrode.

Introduction

There are numerous situations in electrochemistry where application of microelectrodes is helpful and even indispensable. For instance, an extremely low conductivity of a system seems to be a case where the special properties of microelectrodes can be effectively used.^{1–4} High resistance usually originates from a very low salt concentration; this may happen in environmental samples and is rather unavoidable in organic solvents of low dielectric constant, where the solubility of ionic species is limited. Especially demanding situation is that of voltammetry of solvents (in other words, of undiluted redox liquids) where the presence of a sufficient amount of supporting electrolyte is simply impossible. For such systems, the support ratio (the ratio of concentrations of supporting electrolyte and substrate) is usually much smaller than 1. Voltammetric measurements in undiluted redox systems with a regularly sized electrode cannot give readable signals, while a microelectrode can decrease the uncompensated ohmic drop so effectively that well-defined voltammetric waves are obtained.

If a limiting steady-state current (total voltammetric waves) is reached, it can be said that the substrate concentration at the electrode surface drops to zero. Since the electroneutrality in each point of the solution must be preserved, this should lead to the formation at the electrode surface of an ionic microlayer consisting of the ionic product and the available counterion, which is a part of the inert electrolyte.^{4–7} Finally, there should appear a difference in the structure and physical properties between the region adjacent to the electrode surface and the solution bulk. One can expect significant changes in viscosity and conductivity and therefore in diffusion coefficients and the activation energy of diffusion in the ionic layer, which should strongly affect the transport of ions and molecules and should have a substantial influence on the magnitudes of the measured steady-state currents.^{7,8} Also, a considerable density gradient

should appear between the ionic microlayer and the pure solvent, which may generate a gravitational convection at the electrode surface and increase correspondingly the wave height.^{8,9} It is worth noting that the direction of the gravitational-transport gradient would depend not only on the orientation of the electrode versus the Earth's gravitational field but also on whether the diffuse, ionic layer is more or less dense than the solution in the bulk. The changes in the voltammetric wave height caused by the above trends justified the assumptions about formation of ionic layers. Just recently experimental evidence for strong accumulation of ions at the microelectrode surface has been presented.¹⁰ The experiments involved the anodic oxidation of undiluted methanol, which was backed by in-situ Raman spectrometry.

The composition and, in consequence, the properties of an ionic microlayer can be easily modified by changing the counterion present in the solution. Such an action leads to appropriate changes in the viscosity and the activation energy of diffusion.^{7,8}

So far several solvents have been found to give well-defined total, anodic, or cathodic voltammetric waves: nitrobenzene,¹¹ benzonitrile,¹¹ aniline and pyrrole,¹² methanol and other simple alcohols,^{8,13} 4-cyanopyridine,¹⁴ acetophenone,¹⁵ dimethyl sulfoxide,¹⁶ and acetonitrile.¹⁷ In each case, interesting physico-chemical and analytical aspects were found.

Our aim was to investigate a solvent frequently used in electrochemistry: nitromethane. We have also examined electrochemically its homologues: nitroethane and 1-nitropropane. Cathodic voltammetric waves of undiluted nitroalkanes were obtained in the presence of several counterions. Both temperature and gravitational measurements were done. The obtained data were compared to those of ferrocene solutions in nitroalkanes.

Experimental Section

The standard three-electrode arrangement with two platinum coils, which served as the counter and the quasi-reference

* To whom correspondence should be addressed. E-mail: stojek@chem.uw.edu.pl.

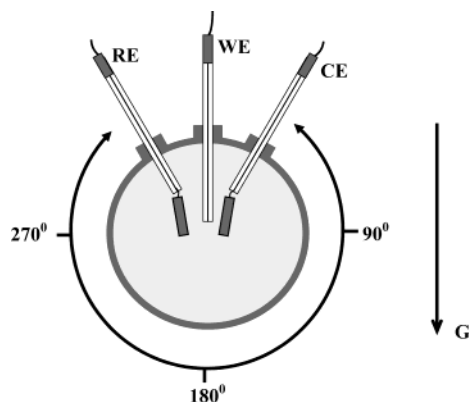


Figure 1. Scheme of the gravitational rotated cell.

electrodes, was employed. The working electrode was a platinum disk microelectrode (nLab, Warsaw) of disk radius 5.3, 11.5, or 25.4 μm . Larger Pt electrodes of radius 50 and 150 μm were also occasionally used. Each time before use, the microelectrodes were polished with 0.3 μm Al_2O_3 powder on a wet pad. After being polished, the electrodes were first rinsed with deionized water obtained from a Milli-Q Plus purification system (Millipore) and then dried with methanol. The surface of the disk was checked occasionally with an Olympus optical microscope, type PME3.

Gravitational studies were performed in a special homemade rotated cell, see Figure 1, that allowed the angle between the direction of the gravitational-force vector and the normal to the surface of the microdisk to be appropriately changed with the accuracy of 1° . The angle $\alpha = 0^\circ$ corresponds to the position of the electrode inserted vertically into the cell; then the normal to the surface and gravitational-field vector have the same directions. The case of opposite direction of the vectors corresponds to $\alpha = 180^\circ$. As it was mentioned above, many intermediate positions ($0 < \alpha < 180$) were possible and applied as well.

An EG & G PARC potentiostat, model 283, was employed during voltammetric measurements and was controlled via ECHEM software. The electrochemical cell was enclosed in an aluminum Faraday's cage.

Nitromethane, nitroethane, and 1-nitropropane were purchased from Aldrich and used as received without preliminary purification. Tetrabutylammonium bromide and tetrahexylammonium bromide (TBABr and THABr, supporting electrolytes) were purchased from Fluka.

Temperature was controlled with a thermostat (Polystat, Cole Parmer) in a special electrochemical water–glycol jacketed cell with the accuracy declared by the manufacturer of 0.01 $^\circ\text{C}$.

Results and Discussion

Voltammograms obtained for undiluted nitromethane (18.53 M), nitroethane (13.85 M), and 1-nitropropane (11.34 M) in the presence of 0.02 M supporting electrolyte (TBABr and THABr) exhibit one very well-defined cathodic wave. Exemplary waves (TBA^+ counterion) are presented in Figure 2. In the range of more negative potentials, there is further increase in the current; however, the current is disturbed and the second wave cannot be formed. This fact is probably related to the evolution of a gas. We are currently doing more research to find out what products are formed within the second wave. In the region of positive potentials, an anodic wave cannot be obtained either.

For both supporting electrolytes and three different microelectrode radii, the obtained chronoamperograms are very stable

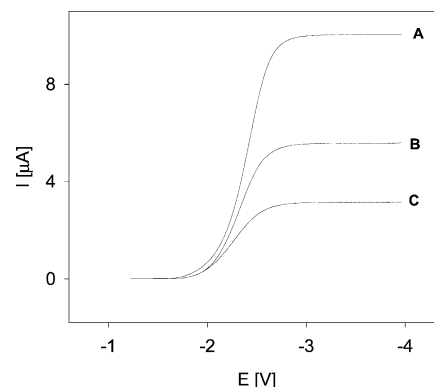


Figure 2. Voltammetric responses of 5.3- μm -radius Pt microdisk in undiluted nitroalkanes: nitromethane (A), nitroethane (B) and 1-nitropropane (C). Supporting electrolyte was 0.02 M TBABr; scan rate = 50 mV/s; $T = 21^\circ\text{C}$.

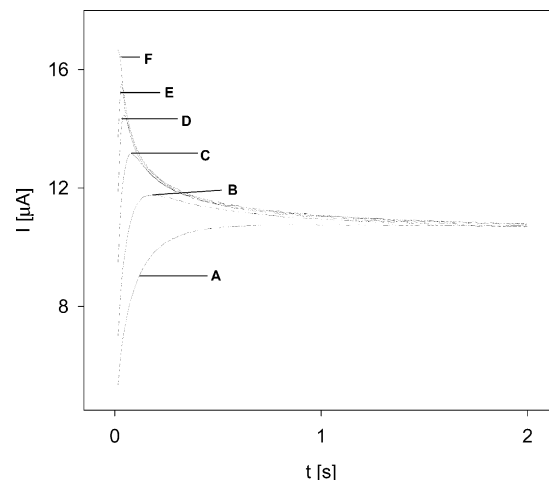


Figure 3. Chronoamperometric responses of 5.3- μm -radius Pt microelectrode in undiluted nitromethane. Applied potential = -2.75 (A), -3.0 (B), -3.25 (C), -3.5 (D), -3.75 (E), and -4.0 V (F). Supporting electrolyte was 0.02 M TBABr; $T = 21^\circ\text{C}$.

and reproducible; the applied potentials were chosen from the range of the wave plateau. An example set of chronoamperograms, only for nitromethane since those for other nitrocompounds are very similar, is shown in Figure 3. The change of the curve shape with potential proves that the current is controlled by diffusion and migration, since there is a good agreement between the experimental data and the theory of chronoamperometry in low support media.¹⁸ The time that is required to attract enough ions to the electrode surface, to build an ionic layer, to compensate ohmic potential drop, and finally to reach the steady-state is a function of supporting electrolyte concentration, electrode radius, and applied potential. The influence of the microelectrode radius is shown in Figure 4: the larger the radius, the higher ohmic drop must be compensated and the longer time is needed to build the ionic layer. It is worth noting here that the final limiting current (steady state) is apparently controlled by the rate of diffusive transport.

Next series of voltammetric experiments involved changing the scan rate, ν , and in fact the change of parameter p , $p = (nF\text{r}_{\text{el}}^2\nu/(RTD_s))^{1/2}$. According to the theory,¹⁹ if the wave height is controlled by the diffusive transport, it should be independent of ν for relatively small values of ν , while it is expected to increase with further increase of ν . The experiments were performed with three microelectrodes of different radius and in the presence of two different inert salts. The dependencies obtained for nitromethane containing 0.02 M TBABr are

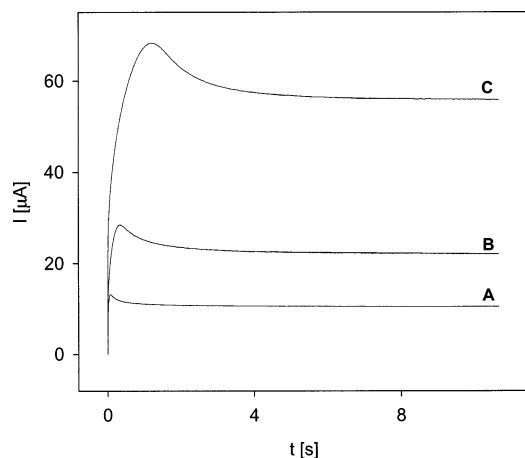


Figure 4. Chronoamperometric responses of undiluted nitromethane obtained with Pt microelectrodes of 5.3 (A), 11.5 (B), and 25.4 μm (C) in radius. Supporting electrolyte was 0.02 M TBABr; applied potential = -3.25 V; $T = 21$ $^{\circ}\text{C}$.

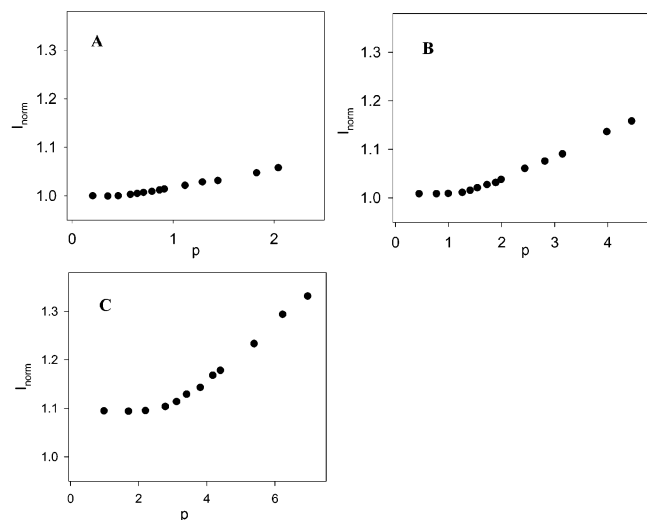


Figure 5. Normalized limiting current for nitromethane plotted versus parameter p defined as $(nF\nu r^2/(DRT))^{1/2}$. Supporting electrolyte was 0.02 M TBABr; scan rate = 10 – 1000 mV/s; Pt microelectrode radius = 5.3 (A), 11.5 (B), and 25.4 μm (C); $T = 21$ $^{\circ}\text{C}$.

presented in Figure 5A–C. They are in agreement with the theory. The wave heights close to the true steady-state current (deviation for nitromethane was found to be 0.8%) could be reached only at the microelectrode of 5 μm in radius and for the slowest scan rate of 10 mV/s. This steady-state limiting current is described with a well-known equation:

$$I_{\text{ss}} = 4nFD_s c_s^b r_{\text{el}} \quad (1)$$

and it enabled us to calculate (after using the iterative approach and correcting appropriately the experimental data for the departure from steady state¹⁹) the values of apparent diffusion coefficients of all nitro-compounds examined in the presence of TBABr and THABr. The values calculated for 25 $^{\circ}\text{C}$ are presented in Table 2. The possible reasons for the differences between the diffusion coefficients is discussed in one of the following sections. The estimated values of D were applied to the eq 1 to calculate the theoretical values of steady-state currents at larger microelectrodes, assuming the number of electrons transferred per nitromethane molecule to be 1 and to normalize the currents in Figure 5. As expected, the normalized current values exceeded 1 in the range of small p for larger

microelectrodes, where some deviations from ideally spherical diffusion occur. At the same time, the range of p where the current dependencies remain almost flat is seemingly a bit longer in the case of THABr compared to that of TBABr; it is due to the smaller apparent diffusion coefficient of nitromethane molecule in the presence of THABr. Since the value of the apparent diffusion coefficient is mostly determined by the physical properties of the ionic microlayer adjacent to the electrode surface, it cannot be identified with the self-diffusion coefficient of the solvent.⁷ Different counterions can affect the viscosity of the depletion layer in a different way and therefore influence the values of D .

The number of electrons that are transferred per one substrate molecule was estimated from the E vs $\ln[(I_{\text{ss}} - I)/I]$ plots. The experimental plots revealed slopes of 0.0617, 0.0658, and 0.0643 V for nitromethane, nitroethane, and 1-nitropropane, respectively. The voltammograms taken for the analysis were obtained using the instrumental compensation of the ohmic drop. Since the theoretical slope for $n = 1$ and $\alpha = 0.5$ equals 0.051 V at 25 $^{\circ}\text{C}$ and the complete compensation of the ohmic drop is rather not possible, our assumption about a one-electron electrode process seems to be justified.

Gravitational Voltammetry. As it was shown in our previous papers concerning alcohols,^{8,9} the generation of an ionic microlayer at the microelectrode surface engenders an additional convective mass flux (natural convection) due to changes of density between the layer and the solution bulk. By changing the position of the microelectrode with respect to the gravitational field's vector, one can modify this additional flux, and this may allow one to make some conclusions on the density of the ionic microlayer.

Angular dependencies of the steady-state current of nitromethane, nitroethane, and 1-nitropropane in the presence of TBABr and THABr have been performed in the range 0° – 180° employing the rotated electrochemical cell. The results for nitromethane and three microelectrodes of different sizes are presented in Figure 6. Irrespective of the position of electrode and added electrolyte, the plateau was very well defined and reproducible for each wave which indicates that the steady-state conditions were easily reached. The influence of the dissolved salt on the magnitude of the angular dependence is evident; however, while it can be neglected for the smallest electrode, it is significant for $r_{\text{el}} = 25.4$ μm where the current increase amounts to ca. 30–60%, which is much more compared to methanol.

Surprisingly, the character of the obtained angular dependences differs very much from that of alcohols.⁸ No maximum is observed at $\alpha = 90^{\circ}$, and the current does not drop below its initial value at the 180° -position. Such behavior must be attributed to a completely different relation between the densities of the depletion layer and the bulk nitroalkane than that concluded for alcohols. We suspect that the electroreduction of the nitro-compounds leads to $\text{ANO}_2^- \text{R}_4\text{N}^+$ electrolyte at the electrode surface (where R denotes either $-(\text{CH}_2)_3\text{CH}_3$ or $-(\text{CH}_2)_5\text{CH}_3$, and A stands for the appropriate alkane) that must be of lower density than the bulk solution. If so, then at the 180° position of electrode, the less dense ionic layer tends to move upward and make the electrode surface more accessible for the substrate. We assume here that the rate of this convective movement of the ionic layer is slower than the rate of its regeneration at the surface, and as a result, the current increases instead of decreasing. Unfortunately the rate of convection and its dependence on electrode size and the angle between the normal to the surface of the disk and the

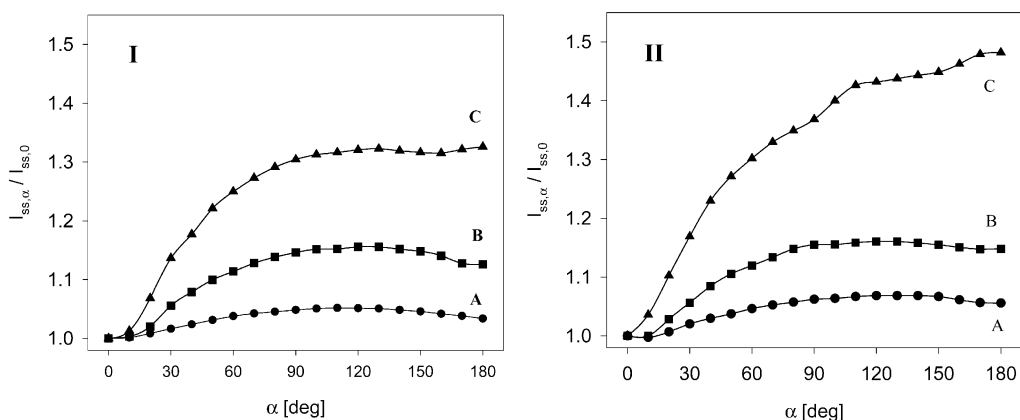


Figure 6. Angular dependencies of steady-state limiting current of undiluted nitromethane. The current was normalized with respect to the limiting current at 0°. Supporting electrolyte was 0.02 M TBABr (I) or 0.02 M THABr (II); scan rate = 50 mV/s; Pt microelectrode radius = 5.3 (A), 11.5 (B), and 25.4 μm (C); $T = 21^\circ\text{C}$.

TABLE 1: Estimated Concentration of Ionic Product and Density of Ionic Layer (Given as the Product of the Concentration of Ionic Product and Its Molar Mass) for Three Nitroalkanes and Two Counterions

R = butyl		R = hexyl		A	density of pure solvent, ANO_2 [g/cm^3]
$C_{(\text{ANO}_2^-)(\text{R}_4\text{N}^+)}$ [mol/dm^3]	$C_{(\text{ANO}_2^-)(\text{R}_4\text{N}^+)}M_{(\text{ANO}_2^-)(\text{R}_4\text{N}^+)}$ [g/cm^3]	$C_{(\text{ANO}_2^-)(\text{R}_4\text{N}^+)}$ [mol/dm^3]	$C_{(\text{ANO}_2^-)(\text{R}_4\text{N}^+)}M_{(\text{ANO}_2^-)(\text{R}_4\text{N}^+)}$ [g/cm^3]		
0.285	0.0853	0.0854	0.0354	methyl	1.134
1.539	0.488	0.495	0.212	ethyl	1.050
3.360	1.112	1.259	0.558	1-propyl	0.998

gravitational vector cannot be predicted easily. In the opposite position, the 0°-position, the ionic layer is blocked by the electrode surface and cannot move upward. Here, some contribution from the buoyancy force can appear as well. The size of the tetraalkylammonium counterion has an extra influence on the magnitude of angular dependence. The currents are higher in the presence of THA^+ (compared to those for TBA^+). Clearly, it can be anticipated that the ionic-liquid-layer density must be lower in the case of THA^+ .

To explain the influence of the counterion size on the density of the ionic layers, some calculations have been done. First, it is clear that the big difference between the sizes of the ANO_2^- and R_4N^+ makes their concentrations within the diffusive ionic layer smaller than half of the bulk solvent concentration. Using the HyperChem software and applying the sphere approximation, we obtained approximate values of the radii of the ionic product and the counterion. Then the concentrations, $C_{\text{ANO}_2^- \text{R}_4\text{N}^+}$, of the ionic liquids generated at the microelectrode surface were estimated and the corresponding densities were calculated as the products of the concentration and the molecular weight: $C_{\text{ANO}_2^- \text{R}_4\text{N}^+}M_{\text{ANO}_2^- \text{R}_4\text{N}^+}$. The results obtained are shown in Table 1. It should be stressed here that the values given in Table 1 are very approximate and rather of mean character, since the ionic layer cannot have identical composition at all distances from the electrode surface. Anyway, it is rather clear that the greater density gradient created in the case of THA^+ than TBA^+ is responsible for the stronger convective flux and is followed by the more pronounced angular dependence of the steady-state current of nitro-compound reduction. This phenomenon can be easily observed in the series nitromethane \rightarrow nitroethane \rightarrow 1-nitropropane: the denser the pure solvent, the greater density gradient is generated during the steady-state conditions and stronger and more pronounced angular dependence is obtained. This is illustrated in Figure 7.

Temperature Experiments. The next set of experiments involved voltammetry of undiluted nitroalkanes in the presence of 5×10^{-3} M TBABr and THABr in a wide range of

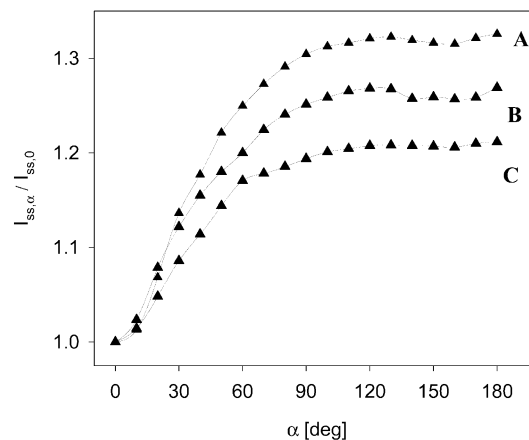


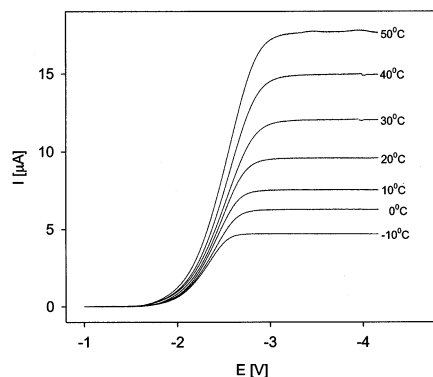
Figure 7. Dependencies of steady-state limiting current for undiluted nitromethane (A), nitroethane (B), and 1-nitropropane (C) vs orientation of the working electrode. Current is normalized with respect to the limiting current at 0°. Supporting electrolyte was 0.02 M TBABr; scan rate = 50 mV/s; Pt microelectrode radius = 25.4 mm; $T = 21^\circ\text{C}$.

temperatures: from -10 to 50°C . For the comparison purpose, similar experiments concerning the oxidation of 2 mM ferrocene in each of the nitroalkanes were done in the presence of 5 mM LiClO_4 . Regardless of the supporting electrolyte and the temperature applied, very stable and reproducible plateaus were obtained for nitroalkanes and ferrocene. Obviously, the wave heights increased gradually with temperature due to the increase in diffusion coefficients of the substrate molecules. In Figure 8, a representative set of voltammograms involving nitromethane is presented. The values of diffusion coefficients of electroactive species in both undiluted and diluted systems were calculated using eq 1 for each temperature and supporting salt. Next, to estimate the activation energy of diffusion, they were plotted according to the Arrhenius method (eq 2):

$$\ln D = \ln D_0 - \frac{1}{R} \frac{E_{\text{activ}}}{T} \quad (2)$$

TABLE 2: Transport Parameters in Depletion Layer during Electroreduction of Undiluted Nitroalkanes

solvent/undiluted substrate (C_{bulk} [M] at 25 °C)	$(D^{(25)} \pm s(D^{(25)})) \times 10^{10}$ [m ² /s]		$(E_{\text{activ}} \pm s(E_{\text{activ}}))$ [kJ/mol]	
	TBABr	THABr	TBABr	THABr
nitromethane (18.53)	2.88 ± 0.01	2.01 ± 0.02	15.67 ± 0.13	16.34 ± 0.06
nitroethane (13.85)	2.29 ± 0.03	1.94 ± 0.03	16.10 ± 0.12	18.52 ± 0.31
1-nitropropane (11.34)	1.55 ± 0.02	1.49 ± 0.02	17.53 ± 0.08	19.25 ± 0.20

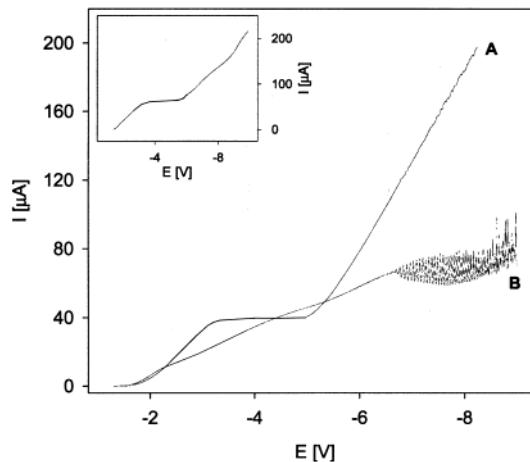
**Figure 8.** Voltammetric responses of 5.3- μm -radius Pt microdisk at various temperatures in undiluted nitromethane. Supporting electrolyte was 5 mM TBABr; scan rate = 50 mV/s.**TABLE 3: Transport Parameters for Electrooxidation of Ferrocene Dissolved in Nitroalkanes**

solvent/undiluted substrate	$(D^{(25)} \pm s(D^{(25)})) \times 10^{10}$ [m ² /s]	$(E_{\text{activ}} \pm s(E_{\text{activ}}))$ [kJ/mol]
	THAClO ₄	THAClO ₄
nitromethane	13.03 ± 0.20	10.40 ± 0.19
nitroethane	12.14 ± 0.19	10.72 ± 0.04
1-nitropropane	11.14 ± 0.17	11.25 ± 0.07

The calculated values of diffusion coefficients and activation energy of diffusion for all electroactive species examined are presented in Tables 2 and 3. The Arrhenius-like plots were perfectly linear with regression coefficients better than 0.996 and relative standard deviations of the slope and the intercept better than 0.8%.

A comparison of the obtained values of the diffusion coefficients and the activation energies of diffusion for nitroalkanes and ferrocene leads to clear conclusions. It is much easier for ferrocene to diffuse in the depletion layer in nitroalkanes as solvents than for nitroalkanes in themselves. For ferrocene, despite the fact that it is a much larger molecule, the diffusion coefficients are bigger by a factor of ca. 4 and the activation energy is substantially smaller, by ca. 40 %. Simply, the depletion layer formed during the electroreduction of undiluted nitroalkanes must be much more viscous. This supports indirectly our claim that this layer is simply ionic. After comparison of the experimentally obtained values of E_{activ} for different counterions, it is striking that it is easier for the nitroalkane molecule to diffuse within the more dense and compact $\text{ANO}_2^- \text{TBA}^+$ layer than in the less dense $\text{ANO}_2^- \text{THA}^+$. Apparently, the layers built of THA^+ are more viscous.

Oscillations. In the successive set of experiments, we have widened the potential window toward very negative values. The primary purpose of this was to check whether the second cathodic wave could be obtained. Instead we have discovered that in the range from -6.5 to -9 V a very interesting phenomenon takes place; the current starts to oscillate. The oscillations were particularly well reproducible at the 25.4 μm electrode. At the smaller electrodes applied in the investigation, the oscillations appeared occasionally. In addition, to get reproducible oscillations, two other conditions must be met. The first one is that the concentration of the supporting electrolyte

**Figure 9.** Voltammetric responses of 25.4- μm -radius Pt microdisk in undiluted nitromethane. Supporting electrolyte was 5 mM THABr; scan rate = 50 mV/s; angle $\alpha = 0^\circ$ (A) and 180° (B). Inset shows response for 0.02 M THABr, scan rate = 50 mV/s, $\alpha = 180^\circ$, and $T = 21^\circ \text{C}$.

should be as low as 5 mM, and the second one requires that the orientation of the microelectrode vs the gravity vector \mathbf{G} is in the range 90° – 180° . The situation is illustrated in Figure 9. Changing appropriately the experimental conditions, either well-defined oscillations (curve B) or a smooth though not very well resolved second wave (inset) can be obtained. Figure 9 also illustrates how effective is the formation of the ionic layer and, at the same time, the drop in the resistance when the orientation of the electrode is 0° (curve A). In this case, the gravitational effect described in the previous part of this paper is stopped. Wave B (orientation 180°) due to the gravitational effect is of much lower slope and higher height. The oscillations are not of identical character in the entire range from 90° to 180° . Near the position of 90° , the oscillations are formed in a narrower potential range, and from ca. 110° , they have the character of that shown in Figure 9. The optimal range of scan rate for getting the best reproducibility of the oscillations has been determined as 50–150 mV/s.

The character of the oscillations can be better examined using chronoamperometry. For this experiment, we have chosen several potentials from the potential range of oscillations and investigated the change of current in time for each selected potential. Typical chronoamperograms are presented in Figure 10. Both the intensity and the frequency of the oscillations increase with negative potential; however, the intensity of oscillations is irregular for potentials more negative than -8 V.

Further increase in the microelectrode size leads to an increase in the intensity of the oscillations; however, the relative intensity (measured vs the reduction current) does not change much and equals ca. 20%, 16%, and 19% for 25.4, 50, and 150 μm electrodes, respectively. The frequency of oscillations decreases with electrode radius. This is illustrated in Figure 11. We think that the change in frequency shown in Figure 11 reflects the changing ability of the system to rebuild the ionic layer.

An analysis of all of the above results made us think that the oscillations in the current are caused by the oscillations in the

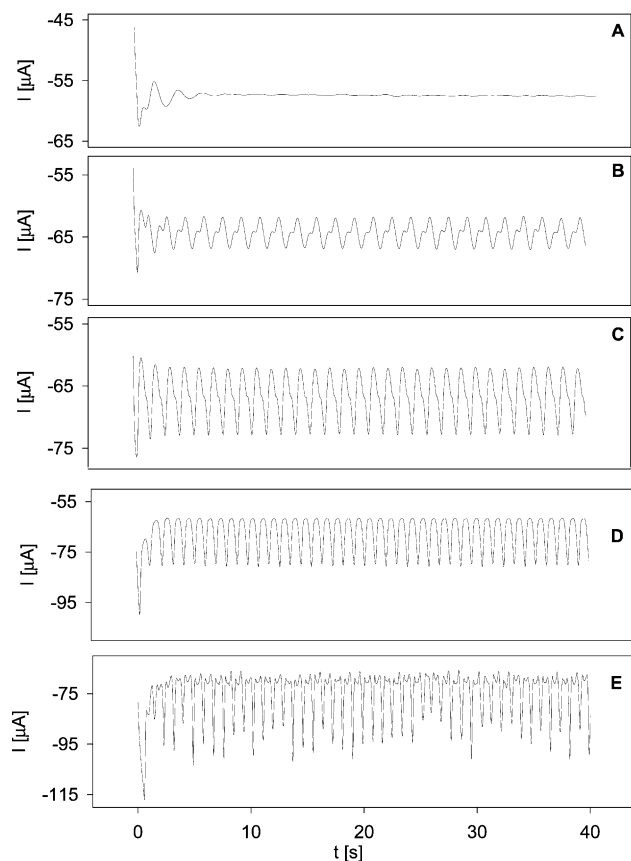


Figure 10. Chronoamperometric responses of 25.4- μm -radius Pt microelectrode in undiluted nitromethane for various potentials applied: -6 (A), -6.5 (B), -7 (C), -8 (D), and -8.5 V (E). Supporting electrolyte was 5 mM THABr; $T = 21^\circ\text{C}$.

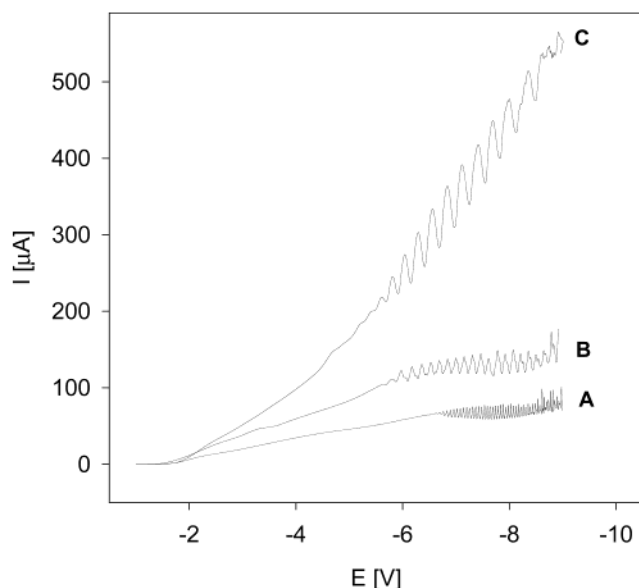


Figure 11. Voltammograms of undiluted nitromethane. Supporting electrolyte was 5 mM THABr; scan rate = 50 mV/s; Pt electrode radius = 25.4 (A), 50 (B), and 150 μm (C); $T = 21^\circ\text{C}$.

total resistance between the working and counter electrodes and therefore by the changes in the ohmic drop and the true potential at the working electrode. To support this conclusion, we have turned to chronopotentiometry. Several current intensities were applied to the electrode, and the resulting electrode potential was measured. The oscillations of the potential measured could exceed 2 V. Typical obtained chronopotentiograms are presented

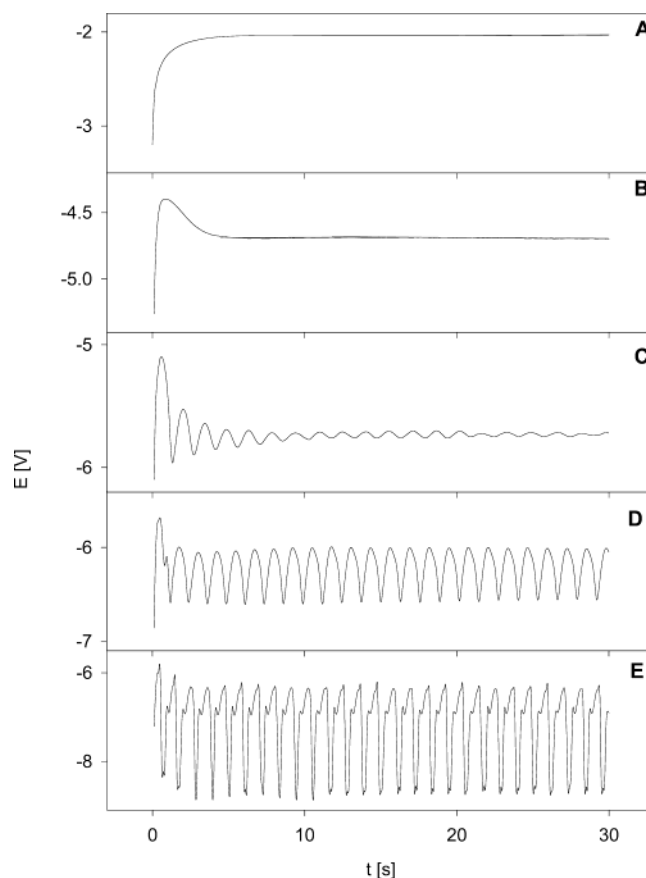


Figure 12. Chronopotentiograms of undiluted nitromethane in 5 mM THABr with $r_{\text{el}} = 25.4 \mu\text{m}$, $T = 21^\circ\text{C}$, and cathodic current = 9.6 (A), 45.6 (B), 59.8 (C), 65 (D), and 75 μA (E).

in Figure 12. Apparently the current oscillations are related to the oscillations in the electrode potential and in the total resistance. A good question here is why an increase in the total resistance takes place while the wave plateau is already reached. Two processes can trigger this phenomenon: either the gravitational removal of an ionic microdrop from the electrode surface or the electroreduction of the counterion accumulated in the ionic layer. As a result of each of these processes, the true electrode potential may drop to a lower value that is not sufficient to maintain the previous current level and where the reduction of the counterion is not possible. After the drop in the current, the rebuilding of the ionic layer occurs and the subsequent rise in the current is seen. The multiple repetition of the above two steps may lead to well-defined oscillations.

Conclusions

Cathodic voltammetry and chronoamperometry done in undiluted nitroalkanes indicate that steady-state limiting current is reached and therefore a microlayer of stable ionic liquid is formed at the microelectrode surface. Since this electroreduction was done in the presence of tetraalkylammonium cations, which were the dominating counterions in the solution, the stoichiometry of the ionic liquid is probably $\text{ANO}_2^-\text{R}_4\text{N}^+$, where R denotes either $-(\text{CH}_2)_3\text{CH}_3$ or $-(\text{CH}_2)_5\text{CH}_3$ and A stands for the appropriate alkane.

The properties of new ionic liquid were estimated by doing some gravitational and temperature measurements. The gravitational experiments showed that the limiting current of undiluted nitroalkanes was higher when the surface of the disk microelectrode was oriented upward. This simply means that the density of the ionic liquid is less than that of pure solvent.

Ionic layer formed starts to move slowly up and triggers an extra transport of the substrate, and we think this leads to a visible enhancement of the current.

The temperature experiments allowed us to determine the activation energy of diffusion of the solvent molecules across the depletion layer. This energy was apparently higher than that of diffusion of the ferrocene molecules in the same solvent. It was higher despite the fact that the ferrocene molecule is much larger. The conclusion reached here is that the depletion layer is much more viscous compared to that in the experiments involving the electrooxidation of ferrocene in nitroalkanes, which is not surprising regarding the ionic liquids.

The appearance of very reproducible oscillations in the range of very negative potentials where the limiting current is already well stabilized was surprising. Since the oscillations were best defined for the 180° orientation of the microelectrode and appeared for both current (chronoamperometry) and electrode potential (chronopotentiometry), they may be related to the gravitational removal of very small drops of ionic liquid from the depletion layer. This should increase the resistance and lower the potential. Correspondingly the current should drop. Next the potential as well as the current should be restored rather quickly. After that a consecutive microdrop would depart upward, and the entire process could be repeated. However, we should admit here that there is another possibility for the explanation of the oscillations: simply they may be triggered by the start of the electroreduction of the counterion. This should also lead to an increase in the resistance in the depletion layer and a drop in the current. And, if the corresponding ohmic drop shifts the potential to the region where the counterion is not

reduced, the ionic layer would be rebuilt and the current would increase. Nevertheless, the gravitational experiments are in favor of the first explanation.

Acknowledgment. This work was supported by Grant 3 T09A 146 19 from KBN, the Polish State Committee for Scientific Research.

References and Notes

- (1) Ciszowska, M.; Stojek, Z. *Anal. Chem.* **2000**, *72*, 754A.
- (2) Amatore, C. *Electrochemistry at Ultramicroelectrodes*. In *Physical Electrochemistry*; Rubinstein, I., Ed.; Marcel Dekker Inc.: New York, 1995.
- (3) Bond, A. M. *Analyst* **1994**, *119*, R1.
- (4) Ciszowska, M.; Stojek, Z. *J. Electroanal. Chem.* **1999**, *466*, 129.
- (5) Stevenson, K. J.; White, H. S. *J. Phys. Chem.* **1996**, *100*, 18818.
- (6) Li, Q.; White, H. S. *Anal. Chem.* **1995**, *67*, 561.
- (7) Hyk, W.; Stojek, Z.; *J. Phys. Chem. B* **1998**, *102*, 577.
- (8) Hyk, W.; Caban, K.; Donten, M.; Stojek, Z. *J. Phys. Chem. B* **2001**, *105*, 6943.
- (9) Caban, K.; Hyk, W.; Stojek, Z. *Chem. Anal. (Warsaw)* **2001**, *46*, 813.
- (10) Caban, K.; Donten, M.; Kudelski, A.; Stojek, Z. *Electrochem. Commun.* **2003**, *5*, 412.
- (11) Malmsten, R. A.; Smith, C. P.; White, H. S. *J. Electroanal. Chem.* **1986**, *215*, 223.
- (12) McCauley, R. A.; Morita, M.; Wilbourn, K. O.; Murray, R. W. *J. Electroanal. Chem.* **1988**, *245*, 321.
- (13) Ciszowska, M.; Stojek, Z. *J. Electroanal. Chem.* **1993**, *344*, 135.
- (14) Morris, R. B.; Fischer, K. F.; White, H. S. *J. Phys. Chem.* **1988**, *92*, 5306.
- (15) Ragsdale, S. R.; Lee, S. R.; Gao, X. P.; White, H. S. *J. Phys. Chem.* **1996**, *100*, 5913.
- (16) Koncka, M.; Stojek, Z. *Electroanalysis* **1995**, *7*, 1010.
- (17) Gadowska, J.; Zieja, J.; Stojek, Z. *Electroanalysis* **2001**, *10*, 621.
- (18) Hyk, W.; Stojek, Z. *J. Electroanal. Chem.* **1996**, *415*, 13.
- (19) Aoki, K.; Akimoto, K.; Tokuda, K.; Matsuda, H.; Osteryoung, J. *J. Electroanal. Chem.* **1984**, *171*, 219.